INTERNATIONAL JOURNAL FOR NUMERICAL METHODS IN FLUIDS, VOL. 7, 1277–1298 (1987)

THE COMPUTATION OF TURBULENT FLOWS OF INDUSTRIAL COMPLEXITY BY THE FINITE ELEMENT METHOD—PROGRESS AND PROSPECTS*

A. G. HUTTON, R. M. SMITH AND S. HICKMOTT

Central Electricity Generating Board, Berkeley Nuclear Laboratories, Berkeley, Glos., U.K.

SUMMARY

This paper is an expanded version of that delivered at the recent Sixth International Symposium on Finite Element Methods in Flow Problems, Antibes, France. It begins by reviewing the role of the finite element method (FEM) in turbulent flow simulation during recent years. The difficulties in incorporating sufficiently general descriptions of turbulence (i.e. two-equation models) into successful finite-element-based Navier–Stokes codes are examined and analysed in some depth. Current progress by various workers in overcoming these difficulties is reviewed and, by concentrating on one particular approach, it is demonstrated that the FEM has now matured into a powerful and flexible tool for solving two-dimensional turbulent flows of industrial complexity. The applications presented highlight those features which render the FEM attractive in this field (viz., minimal false diffusion, arbitrary local refinement, boundary fitting capabilities and non-structured grids). Finally, the prospects and challenges for the future are briefly discussed. In particular, the urgency and difficulty of constructing a competitive three-dimensional capability which preserves these features is examined.

KEY WORDS Review Article Industrial Flow Finite Element Turbulent Flow k–ε Turbulence Model

INTRODUCTION

In recent years, the impact of the finite element method (FEM) upon many aspects of computational fluid dynamics (CFD), a field of endeavour which is traditionally dominated by finite difference/finite volume techniques, has been steadily increasing.[1] For example, a survey of the recent literature will reveal that the FEM is now used regularly to solve problems of industrial complexity in applications such as coastal and estuarial hydrodynamics, oil reservoir modelling, compressible aerodynamics and fluid–structure interaction.[2–4] As recently pointed out by one of the authors,[5] the glaring exception seems to be turbulent flow and heat transfer. This is illustrated in Figure 1, in which the percentages of papers appearing in the Proceedings of recent CFD Conferences which deal with (i) turbulent flow using the FEM, (ii) turbulent flow using finite volume and (iii) general viscous flow using the FEM are presented. Although the data from the cited Conferences are not comparable in absolute terms, certain trends are apparent. As can be seen, the FEM has and continues to exert a significant impact upon general viscous flow computation, demonstrating to great effect various advanced (second-generation) features such as negligible false diffusion, fitting of awkward boundary shapes and arbitrary local refinement with non-structured

* Based on an invited lecture.

0271–2091/87/111277–22$11.00

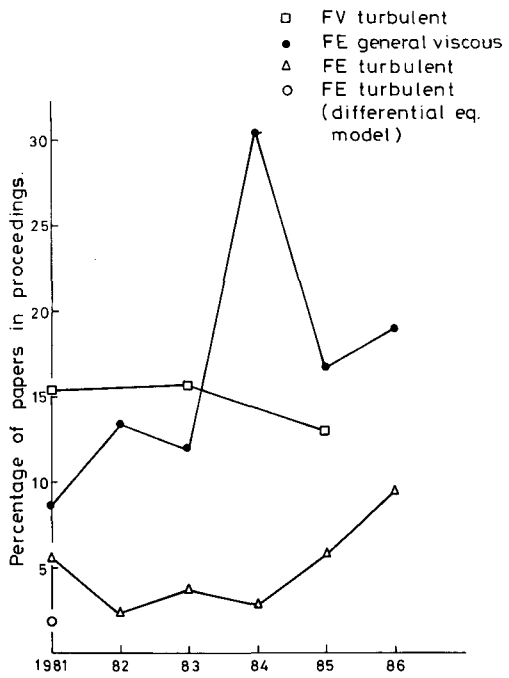

Figure 1. The impact of the FEM on turbulent and general viscous flow computation (even years—Finite Elements in Flow Problems; odd years—Numerical Methods in Laminar and Turbulent Flow)

grids. The impact upon turbulent flow computation has by comparison been disappointing (although the upturn in the curve suggested by the Antibes Conference,[4] if sustained, is encouraging). And yet, turbulent flow is by far the more important area as far as industrial application is concerned and, indeed, is an area which should benefit enormously from the above-mentioned 'second-generation' features of the FEM. It is, then, somewhat surprising that to date the FEM has played such a minor role.

In the wake of the successful experience with viscous flow simulation, initial activity was high. Figure 1 indicates that, at that time (*circa* 1981), the percentage of FE papers dealing with turbulent flow was at the same level as in 1985. However, most of these addressed fairly simple uni-directional flows employing simple algebraic prescriptions of the effective viscosity. Only a third dealt with the more complex geometries requiring differential equation turbulence models. By 1982 the overall level of activity had fallen dramatically and has remained fairly low until very recently. The reason seems to be due to difficulties which are encountered when incorporating sufficiently general descriptions of turbulence into that FE framework which has been developed for general viscous flows, while retaining a similar degree of robustness.[6–10]

An increasing number of workers have been addressing these difficulties with considerable energy in recent years. Others, with a background in finite differences, are endeavouring to graft this established technology into the FE context.[11,12] In short, the level of activity is increasing and it would seem that progress is being made (witness the 1986 upturn in Figure 1). It is, therefore, perhaps timely to attempt a review of the current state of the art.

Having set down the basic equations which are generally used to simulate industrial flows, the paper will continue by examining the nature and cause of the difficulties that have been encountered. The various options that are currently being pursued to overcome these difficulties will then be briefly surveyed before presenting some applications (based upon one of these options)

which demonstrate that the FEM is now being used to solve problems of industrial complexity and which underline those 'second-generation' features which render the method so attractive. Finally, the paper will conclude with one or two speculative comments on the challenges and prospects for the future.

BASIC EQUATIONS FOR PRACTICAL TURBULENT FLOW COMPUTATION

Differential equations

Attention will be restricted to 'time-meaned' formulations of turbulent flow. That is to say, all dependent variables appearing in the equations are presumed to represent an integrated average over a time interval which is long compared to the timescale of the largest eddy, but short compared to the timescale of flow evolution imposed by the boundary conditions. Whether or not such a time interval can be sensibly defined will not be debated here, since the primary concern will be with the computation of 'time-meaned steady' flows, the evolutionary terms being retained only for the purpose of numerical convenience in seeking this steady state.

For simplicity, only two-dimensional flows will be considered (the instantaneous flow is of course three-dimensional). Let u_1, u_2 represent the mean velocity components in the co-ordinate directions x_1, x_2 respectively and let p represent the mean pressure. Then if all variables are rendered dimensionless with respect to a characteristic velocity and length, the momentum and continuity equations can be written

$$\frac{\partial u_n}{\partial t} + u_m \frac{\partial u_n}{\partial x_m} + \frac{\partial p}{\partial x_n} - \frac{1}{x_2^\alpha}\frac{\partial}{\partial x_m}(x_2^\alpha \tau_{mn}) + 2\alpha \frac{1+\mu_T}{Re}\frac{u_2}{x_2^2}\delta_{n2} = B_n, \tag{1}$$

$$\frac{1}{x_2^\alpha}\frac{\partial}{\partial x_m}(x_2^\alpha u_m) = 0, \tag{2}$$

$$\tau_{mn} = \frac{1+\mu_T}{Re}\left(\frac{\partial u_m}{\partial x_n} + \frac{\partial u_n}{\partial x_m}\right). \tag{3}$$

Here Re denotes the Reynolds number, B_n are the components of a body force (e.g. buoyancy or Lorentz force) and the parameter α takes the value zero for two-dimensional planar flows and unity for axisymmetric flows (in which case u_2 is the radial velocity component). For most of the flow situations encountered in practice, the turbulence structure is not everywhere locally determined (e.g. separation, reattachment, bodies of recirculating fluid, etc.) and thus the turbulent viscosity μ_T must be constructed from additional transport equations governing the velocity and length scales of the larger turbulent eddies. The simplest and certainly the most popular closure at this level is the k–ε model, where k is the turbulence energy and ε is its rate of dissipation. According to this prescription

$$\mu_T/Re = C_\mu k^2/\varepsilon, \tag{4}$$

$$\frac{\partial k}{\partial t} + u_m \frac{\partial k}{\partial x_m} - \frac{1}{Re}\frac{1}{x_2^\alpha}\frac{\partial}{\partial x_m}\left(\frac{x_2^\alpha \mu_T}{\sigma_k}\frac{\partial k}{\partial x_m}\right) = \frac{\mu_T}{Re}S_u - \varepsilon, \tag{5}$$

$$\frac{\partial \varepsilon}{\partial t} + u_m \frac{\partial \varepsilon}{\partial x_m} - \frac{1}{Re}\frac{1}{x_2^\alpha}\frac{\partial}{\partial x_m}\left(\frac{x_2^\alpha \mu_T}{\sigma_\varepsilon}\frac{\partial \varepsilon}{\partial x_m}\right) = C_\mu C_{1\varepsilon} k S_u - C_{2\varepsilon}\frac{\varepsilon^2}{k}, \tag{6}$$

$$S_u = \left(\frac{\partial u_n}{\partial x_m} + \frac{\partial u_m}{\partial x_n}\right)\frac{\partial u_n}{\partial x_m} + 2\alpha\left(\frac{u_2}{x_2}\right)^2, \tag{7}$$

where $C_\mu, \sigma_k, \sigma_\varepsilon, C_{1\varepsilon}$ and $C_{2\varepsilon}$ are model constants, usually set to the recommended standard values 0·09, 1·0, 1·3, 1·44 and 1·92 respectively.

From equation (3) it is apparent that only those flows where the turbulent stresses can be interpreted by means of a scalar turbulent viscosity are considered. While this might seem unduly restrictive, the model nonetheless proves adequate for many engineering purposes[13] and currently forms the basis of most industrial applications. Furthermore, in those situations where higher-order closures are required to capture the essential physics, equations (5) and (6) invariably remain at the heart of the model.[13,14] In short, effective means of treating these equations is crucial at all levels of practical simulation.

Boundary conditions

In implementing the above equations into a numerical scheme, the solution is not usually extended right to a wall but is instead matched to universal wall functions describing the behaviour of flow at some small distance h from the wall. This avoids the requirement for excessive grid refinement in the wall vicinity and also having to deal with viscous effects in the turbulence model.

Thus, if u, v represent tangential and normal components respectively and subscript h denotes a quantity evaluated at distance h from the wall, it is assumed

$$\frac{u_h}{u_\tau} = \frac{1}{\kappa} \ln (Re\, u_\tau h) + C, \quad Re\, u_\tau h > 30, \tag{8}$$

$$v_h = 0, \tag{9}$$

$$k_h = \tau_w / C_\mu^{1/2}, \tag{10}$$

$$\varepsilon_h = C_\mu^{3/4} k_h^{3/2} / \kappa h, \tag{11}$$

where τ_w denotes the (dimensionless) wall shear stress, κ and C are universal constants and the scale velocity u_τ is given as $\tau_w^{1/2}$. Some practitioners (in fact, probably most)[15,16] use the alternative definition for u_τ,

$$u_\tau = C_\mu^{1/4} k_h^{1/2}, \tag{12}$$

with equation (8) then being written

$$\frac{u_h u_\tau}{\tau_w} = \frac{1}{\kappa} \ln (Re\, u_\tau h) + C, \quad Re\, u_\tau h > 30. \tag{13}$$

Equation (10) (which is a statement that the turbulence is in local equilibrium) renders the two forms identical. If, however, equation (10) is replaced by the Neumann condition $(\partial k / \partial n)_h = 0$, then the equivalence is broken and distinct numerical advantages can ensue from adopting equations (12) and (13). Various wall regions of flow are encountered for which the turbulence is not in local equilibrium (e.g., the vicinity of a reattachment point at which τ_w is zero). Difficulties arise in applying equation (8) in such regions, since $Re \tau_w^{1/2} h$ is small, and one is then normally forced to revert to the viscous asymptote[17]

$$u_h / u_\tau = Re\, u_\tau h,$$

even though the turbulence model cannot strictly span such behaviour. Furthermore, if heat transfer is being calculated using thermal-momentum similarity, the predicted heat transfer coefficient will exhibit a minimum at reattachment instead of a maximum as experimentally oberved. On the other hand levels of k remain high if the Neumann condition is adopted so that

there is usually no difficulty in applying equation (13) with u_τ given by equation (12). This also produces the (qualitatively) correct heat transfer behaviour.

The other types of boundary commonly encountered are treated in a now standard way. At inlets all dependent variables except pressure are specified, whereas at symmetry lines

$$\mathbf{u}\cdot\mathbf{n} = 0, \quad \frac{\partial k}{\partial n} = \frac{\partial \varepsilon}{\partial n} = \frac{\partial \mathbf{u}\cdot\mathbf{t}}{\partial n} = 0.$$

where $\mathbf{n}, \mathbf{t}$ are the unit normal and tangential vectors respectively. It is usual to leave the dependent variables unspecified at outlets, thus approximating the natural boundary conditions

$$\frac{\partial k}{\partial n} = \frac{\partial \varepsilon}{\partial n} = (-p\delta_{mn} + \tau_{mn})n_m = 0.$$

EXPERIENCE WITH GALERKIN FINITE ELEMENT DISCRETIZATION

Discretization

If in equations (1) and (3) μ_T is specified explicitly, then the equation system is identical to that describing a variable-viscosity laminar flow. Such laminar flows have been successfully treated using what are now standard techniques for the Navier–Stokes system.[18,19] Typically the flow region is covered with a structure of triangular or quadrilateral elements. On each of these the velocity is quadratically or perhaps linearly interpolated and solutions to the momentum equations are then sought by the Galerkin method of approximation using symmetric weighting (i.e., no upwinding). The continuity equation is incorporated either by the penalty method[19,20] (in which case the explicit appearance of pressure is suppressed) or by the Lagrange multiplier method[19] (the pressure then being linear or piecewise constant over quadratic or linear velocity elements respectively) or a combination of both (e.g., the PALM method[21]). If steady-state solutions are sought (the primary concern of this paper), it is usual to remove the time variation and tackle the resulting equation set using the Newton–Raphson (NR) iterative procedure coupled with a direct frontal solver for the linear systems within each iteration. Once a wall treatment based upon the procedures outlined above is incorporated, such schemes also prove successful in calculating turbulent flows for which μ_T is algebraically specified. It thus seemed natural, when extending the methodology to handle complex turbulent flows, to discretize equations (5) and (6) using a similar Galerkin finite element treatment, with k and ε typically expanded in terms of the velocity basis functions. Although this approach proved initially successful for simple unidirectional flows[22,23] (witness the 1981 level of activity in Figure 1), several authors have reported difficulties when more complex configurations were attempted.

A survey of the difficulties

Some of the earliest attempts to apply GFE methods to the k–ε system in complex configurations were those of Larock and his co-workers. Larock and Schamber[6] presented solutions for recirculating flow in a sedimentation basin. These were obtained by directly tackling the stationary equation set by employing a strategy which alternated between velocity field updates for a given μ_T variation and μ_T updates (via the k–ε coupled system) for a given velocity field. Special relaxation procedures and modifications to the Newton–Raphson (NR) scheme were employed for treating the k–ε system in order to avoid the appearance of negative values of k and ε, since these inevitably

led to divergence. Even so, the stability of the scheme proved oversensitive to the quality of the initialization (i.e. its 'closeness' to the solution) and was therefore considered impractical as a general tool.

Subsequent work has endeavoured to improve the robustness of the scheme.[24] This is achieved by the introduction of line searching (negative k and ε values are disallowed in the search) and by 'homing in' on the k–ε solution for a given velocity update by switching progressively through three distinct algorithms, each one introducing more non-linearity (i.e., implicitness) than its predecessor. Obviously a complex iteration schedule (i.e., set of instructions for switching between equation sets and between algorithms) must be specified to operate the scheme and at present this is done largely by trial and error. Operational experience indicates the desirability of further research in this area.

Tong[7] investigated the performance of a GFE scheme for solving flow over a backward-facing step. An alternating outer iteration strategy like that of Larock and Schamber was employed, except that the k–ε system was solved by a Picard- rather than a NR-based scheme. Solutions were obtained from crude initializations (zero velocity, constant μ_T, k and ε) but only after introducing special procedures which essentially altered the system being solved. In particular, the values of the model constants σ_k, σ_ε were reduced to 0·5 (this is equivalent to introducing false diffusion in the k and ε equations), only the absolute values of k and ε were accepted after each Picard update and the velocity field was successively updated without convergence in k and ε being achieved. Tong, in an attempt to justify the second of these rather *ad hoc* procedures, suggested that the tendency to produce negative values of ε signified an unphysical transfer of energy from small to large wavelengths. This, in his opinion, was an expected consequence of the two-dimensional nature of the k–ε formulation, since the transfer of energy through the spectrum was in reality via a three-dimensional mechanism. It was therefore necessary and physically plausible to reject negative values in order to 'enforce a forward energy cascade'.

Polansky *et al.*[9] employed GFE approximations on quadratic triangular elements to calculate separated flow over a backward-facing step at a fairly low Reynolds number of 3025 (based on step height and upstream velocity). Once again, the system was partitioned into turbulent and dynamical subsystems, each being updated successively by NR iteration. In order to stabilize the scheme, a large component of artificial turbulent viscosity was introduced, this being progressively reduced as the iterations advanced, and the non-linear terms in the equations were introduced only gradually. Despite this, they found it necessary to dispense with wall functions (i.e., extend the grid to the wall) and to introduce a low-Reynolds-number turbulence model in order to achieve convergence.

Considerable insight into the cause and nature of such difficulties was provided by Smith,[8] who studied flow through a sudden pipe expansion at a Reynolds number of 3×10^4 (based upon downstream pipe diameter and bulk velocity). In his model, the source quantity S_u (equation (7)) was introduced explicitly as an interpolated variable with quadratic representation over the elements. Nodal values of S_u were determined by GFE approximation to equation (7) and these were then introduced into a GFE treatment of the steady-state form of equations (5) and (6) in which the right-hand sides, as a whole, were quadratically interpolated over each element. Careful numerical experimentation revealed that, at least for the boundary conditions adopted (viz., inlet located at the step position and wall functions used in the lee of the step), no solution existed to the resulting system on the mesh chosen. This was because the velocity field in the vicinity on the re-entrant corner was such as to produce an extremely sharp peak in S_u. In response to this peak, k and ε increased exponentially with distance from the corner until k^2/ε was large enough for diffusion to reverse the trend (see equation (4)). The grid was not sufficient to resolve this growth and decay (i.e., peak) and spatial oscillations characteristic of the GFE method thus ensued. Once these were of

sufficient amplitude to produce negative values in k and ε (which invariably proved the case), a real solution no longer existed since diffusivities became negative (equation (4)) and sources and sinks reversed their roles (equations (5) and (6)). Local grid refinement only exacerbated the situation by sharpening the peak in S_u and thus the response of k and ε. In fact, a grid sufficient to capture this response and thus stabilize the scheme could not apparently be constructed. This raises the question what, if any, is the limiting value of S_u with grid refinement. As can be seen from equation (7), S_u is a quadratic function of velocity gradients and, in particular, the square of the radial derivative of the axial component. As the corner is approached, this can be approximated by $(\Delta u/\Delta r)^2$, where Δu is the velocity change across the shear layer emanating from the step and Δr or its radial thickness. In physical reality, this ratio is undoubtedly large as Δr diminishes. However, in the Smith calculation, its value was determined by the imposed boundary conditions at the (inlet) grid edge. The velocity at the first node above the step was imposed from experiment, whereas the velocity at the first node below the corner was imposed by the wall functions. These two distinct behaviours produce a finite Δu between these nodes irrespective of their spacing, say Δr, and consequently S_u is unlikely to be bounded as the grid is refined.

This problem, which it should be emphasized is only local in character, could possibly have been alleviated by removing the inlet to a position upstream of the step and/or dispensing with wall functions (cf. Polansky *et al.*[9]). However, a robust general purpose code should be capable of dealing with any well-posed boundary condition and indeed any physical distribution of sources, at least in the sense of producing a solution on a given grid. A naive extension of the GFE discretization to the k–ε system will not exhibit robustness in this sense, although, of course, there will be many cases where solutions can be found. For the general situation, the key elements in ensuring a solution on a given grid are the introduction of false diffusion to attenuate the response of k and ε in regions of high net production and/or a judicious representation of S_u on the elements (i.e., a smoother resolution of S_u so that local peaks are reduced). Smith showed that, by adopting this latter option and representing S_u as a constant on each element, a discrete solution could indeed be obtained. Unfortunately, the existence of a discrete solution does not guarantee that the chosen solver will find it. The Newton–Raphson scheme employed by Smith converged only if presented with an extremely accurate initial guess (e.g., a finite difference solution). It was established that this behaviour was due to the presence of multiple false minima in the vicinity of the required solution. A large-stepping, implicit solver such as NR is obviously not ideal in such situations, despite its success in treating laminar flows.

Less troublesome experiences

It should be pointed out at this juncture that several authors have published GFE solutions to complex turbulent flows without reporting any particular difficulties.[14,17,25–27]

Baker[27] has concentrated on essentially three-dimensional parabolic flows. For example, Baker and Orzechowski[14] solved turbulent flow in the region formed by the intersection of two aerodynamic surfaces (e.g., wing–fuselage). Such flows are essentially uni-directional in nature, with comparatively weak secondary recirculations normal to the main flow direction. Although they present special difficulties in modelling the turbulence structure (a simple scalar μ_T will not suffice), the ingredients which give rise to the difficulties discussed above are largely absent (i.e., strongly elliptic flows with intense regions of shear).

However, these ingredients are present in several other publications. For example, Taylor *et al.*[17] and Uchida[25] both report solutions to the same downstream-facing step configuration as that tackled by Polanski *et al.*[9] (as discussed above). Taylor *et al.* tackled the steady equations directly, partitioning them into two sets, the first comprising the momentum and k equations (the latter

being in the well-known one-equation k–l form), the second comprising the ε equation. Each set was linearized by successive substitution rather than Newton–Raphson with under-relaxation between iterations. The solution procedure alternated between solutions of the first set and l updates via the second set ($\mathbf{u}, k$ fixed). Uchida opted for a transient GFE formulation in which the velocity–pressure variables were replaced by the vorticity–stream function. The steady solution was sought by a procedure in which each equation in the ω, ψ, k and ε set was linearized using current (nth level) time values and then advancing to the $(n+1)$th level by means of Crank–Nicolson time-stepping. Neither author reported any particular difficulty in obtaining convergence. This, at first sight, may seem at odds with the difficulties reported in the foregoing discussion. However, it must be recognized that the Reynolds number was fairly low (3025) and in both cases solutions were started well upstream of the step. These factors afford a considerable alleviation of the problems encountered by Smith, although not those reported by Polansky *et al.* A key to Uchida's success could be the time-stepping technique used for solving the equations and the fact that the velocity field is derived from the stream function, so that S_u is very crudely represented on each element. Also, it is interesting to note that Taylor *et al.* calculated the reattachment length to be less than $4{\cdot}5h$(h is the step height) and Uchida produced the figure $3{\cdot}3h$. The experimentally observed value is $6h$ and the k–ε model, despite its tendency to overpredict length scale near reattachment, should produce a value in excess of $5h$.[28] Indeed, Polansky *et al.*, albeit with their low-Reynolds-number version of k–ε, calculated reattachment at $5{\cdot}5h$. If, as this suggests, the two schemes under discussion[17,25] were overdiffusive, their robustness would be considerably enhanced.

OVERCOMING THE DIFFICULTIES

From the above-related experiences, it would seem that any code based upon the k–ε model which is also sufficiently robust to tackle a large range of flows of industrial complexity must incorporate a judicious representation of the sources in relation to the $\mathbf{u}$ field and/or a degree of false diffusion to ensure that a solution exists on practical grids (i.e., negative k and ε values are precluded). In addition, an iterative solver of large radius of convergence is required; that is, a gentle relaxation procedure which can 'home in' on the solution, ignoring false minima and avoiding non-physical regions. It is of interest to note that most finite volume codes in current widespread use possess all three ingredients in large measure, which perhaps explains their popularity in industrial application. Indeed, attempts to refine the modelling (e.g., the introduction of skew upwind differencing or QUICK into the k–ε equations) prove difficult due to exactly those problems encountered by GFE.[28,29]

Current progress with the FEM

Betts and Haroutunian[29] have proposed a FE formulation with several of these ingredients and have successfully applied it to flow over a backward-facing step and a model of the atmospheric surface layer. The formulation is based upon the methods of Gresho *et al.*[30] so that the transient rather than the steady equations are tackled. Over each element, the $\mathbf{u}$, k and ε fields are linearly or bilinearly represented, whereas p is piecewise constant. The discretization is effected by Galerkin approximation (although, unlike Gresho, 2×2 point quadrature is used) and the solution is obtained through explicit Euler time-marching to the steady state. In order to stabilize this procedure, a 'balancing tensor diffusivity' is introduced which, for finite time steps, is still active when the steady state is achieved. Consequently, (stabilising) numerical diffusion acting only along the streamline direction is introduced for all variables, the diffusivities being proportional to $C\Gamma_h$,

where C is the Courant number and Γ_h is the local grid Peclet or Reynolds number. This feature, together with the time-marching procedure (equivalent to an explicit relaxation technique), renders the scheme comparatively robust and thus an attractive base for industrial computation. However, this is achieved with the penalty of some curtailment of the FEM second-generation features. Apart from the introduction of false (streamline) diffusion on all variables, the degree of local refinement which can be afforded is limited by the stability bound on the Courant number.

Benqué and his co-workers at Electricité de France–LNH have pioneered the development of FE-based split operator techniques, convection being treated by the characteristic–Galerkin method.[31] The essential principles of this approach can be simply explained by considering the scalar transport equation

$$\frac{\mathrm{D}\theta}{\mathrm{D}t} = \frac{\partial\theta}{\partial t} + u_m \frac{\partial\theta}{\partial x_m} = \frac{1}{Re}\frac{1}{x_2^{\alpha}}\frac{\partial}{\partial x_m}\left(x_2^{\alpha}\frac{\mu_{\mathrm{T}}}{\sigma_\theta}\frac{\partial\theta}{\partial x_m}\right) + S_\theta. \tag{14}$$

Equations (1) (provided μ_{T} is a constant), (5) and (6) are of this general form. If a space of time-dependent weighting functions $\psi(\mathbf{x}, t)$ is employed to convert equation (14) into an integral formulation, then in the usual Galerkin fashion, at any instant t,

$$\int_\Omega \frac{\mathrm{D}\theta}{\mathrm{D}t}\psi\,\mathrm{d}\mathbf{x} = -\int_\Omega \frac{\mu_{\mathrm{T}}}{\sigma_\theta Re}\frac{\partial\theta}{\partial x_m}\frac{\partial\psi}{\partial x_m}\mathrm{d}\mathbf{x} + \int_\Omega S_\theta\psi\,\mathrm{d}\mathbf{x}. \tag{15}$$

If, now, equation (15) is integrated in time over the interval (t_n, t_{n+1}), we obtain

$$\begin{aligned}\int_{t_n}^{t_{n+1}}\int_\Omega \frac{\mathrm{D}\theta}{\mathrm{D}t}\psi\,\mathrm{d}\mathbf{x}\,\mathrm{d}t &= \int_{t_n}^{t_{n+1}}\frac{\mathrm{D}}{\mathrm{D}t}\int_\Omega \theta\psi\,\mathrm{d}\mathbf{x}\,\mathrm{d}t - \int_{t_n}^{t_{n+1}}\int_\Omega \theta\frac{\mathrm{D}\psi}{\mathrm{D}t}\mathrm{d}\mathbf{x}\,\mathrm{d}t \\ &= \int_{t_n}^{t_{n+1}}\left(-\int_\Omega \frac{\mu_{\mathrm{T}}}{\sigma_\theta Re}\frac{\partial\theta}{\partial x_m}\frac{\partial\psi}{\partial x_m}\mathrm{d}\mathbf{x} + \int_\Omega S_\theta\psi\,\mathrm{d}\mathbf{x}\right)\mathrm{d}t.\end{aligned} \tag{16}$$

The key to the method is now to choose functions ψ such that $\mathrm{D}\psi/\mathrm{D}t = 0$ on (t_n, t_{n+1}). Equation (16) then reduces to the much simplified form

$$\left(\int_\Omega \theta\psi\,\mathrm{d}\mathbf{x}\right)^{n+1} - \left(\int_\Omega \theta\psi\,\mathrm{d}\mathbf{x}\right)^{n} = \int_{t_n}^{t_{n+1}}\left(-\int_\Omega \frac{\mu_{\mathrm{T}}}{\sigma_\theta Re}\frac{\partial\theta}{\partial x_m}\frac{\partial\psi}{\partial x_m}\mathrm{d}\mathbf{x} + \int_\Omega S_\theta\psi\,\mathrm{d}\mathbf{x}\right)\mathrm{d}t, \tag{17}$$

which can be discretized in time, typically by trapezoidal integration, to form a fairly simple, implicit algorithm for $(n+1)$th time level values of θ. The choice of ψ such that $\mathrm{D}\psi/\mathrm{D}t = 0$ implies that ψ is independent of time in a frame moving with the fluid particles; that is, the weighting functions are transported along the streamlines. These functions are constructed as follows. A finite element spatial discretization is introduced and the functions at time $t = t_{n+1}$ are defined to be the usual element basis functions on this grid. At time $t = t_n$, they are the basis functions on a grid formed by moving the nodal points back along the streamlines to the positions they would have occupied (at $t = t_n$) if they were fluid particles. When the method is applied to the momentum equations (constant μ_{T}), equation (17) represents a generalized Stokes problem, θ representing each of the velocity components. This is handled using the preconditioned conjugate gradient Uzawa algorithm.[32] When a turbulence model such as k–ε is introduced, the velocity components can no longer be formally decoupled due to the spatially varying μ_{T} and the cross-coupling introduced by the wall functions. However, these difficulties have been resolved and the method has been successfully applied to several complex flows.[32] As before, the key to robustness is the action of numerical diffusion along the streamline direction and a time-marching technique for 'homing in' on the solution. Unlike the previous formulation, the scheme is unconditionally stable

and thus there is, in principle, no restriction imposed on the degree of local refinement which can be introduced. However, improved local resolution of the solution (the primary purpose of local refinement) may not ensue without a concomitant reduction in the time step.

Brison *et al.*[33] introduced a formulation, further developed in reference 34, in which the momentum equations are advanced through time using a semi-implicit fractional time-stepping technique. The first (fractional) step handles convection, thus producing a generalized Stokes problem for the second (fractional) step. The k and ε equations are each advanced by a single implicit time step. Streamline upwinding in the manner of Hughes and Brooks[35] is introduced into all equations. The method has been successfully applied to jets and flow over a backward-facing step at a Reynolds number of $4{\cdot}5 \times 10^4$. It is claimed that the algorithm is unconditionally stable consequently there is no practical restriction on the degree of local refinement which can be introduced. However, as pointed out above, such unconditional stability may be achieved at the expense of local accuracy on highly refined grids. For example, the recirculation length calculated by Brison *et al.* was $5{\cdot}33h$, whereas, for the same problem, Betts and Haroutunian, using an explicit time-stepping scheme, produced a value $6{\cdot}23h$. The experimentally measured value was $7{\cdot}0h \pm 0{\cdot}5h$.

Coulon and Magnaud[36] have successfully applied a similar technique to a pipe expansion problem with experimentally provided data set at an inlet just downstream of the expansion. Once again, the key to success appears to be the adoption of a transient algorithm incorporating streamline diffusion.[35]

Benim and Zinser[16] have solved the same problem (albeit with a much larger expansion ratio) by tackling the steady equations directly. They adopted a strategy which alternated between dynamical and turbulence equation sets, each being solved implicitly within iterations. Unfortunately, few details of the scheme are provided in Reference 16. Its stability seems due, in large part, to under-relaxation of the updated field variables and the introduction of the Hughes quadrature upwind scheme[35] (this is more diffusive than streamline upwinding).

Another approach which avoids time-stepping has been proposed in Reference 15. This also avoids reliance upon upwinding, so that the algorithm lies much closer to the original GFE treatment of the Navier–Stokes equations (viz., no limitation on grid designs and formally free of numerical diffusion). As already pointed out, Smith has shown that, if the representation of S_u over an element is judiciously chosen (e.g., S_u a constant), then a solution to the discrete system exists for the most exacting of cases without resorting to upwind weighting or the explicit inclusion of numerical diffusion. Unfortunately, this solution is difficult to locate, especially using implicit non-linear solvers such as NR-based schemes. It transpires that this problem is considerably eased by adopting an alternative description of the turbulence based upon $q(\equiv k^{1/2})$ and f (a frequency of the large-scale motions) rather than k and ε.[15,21] This approach will now be examined in some detail, since it forms the basis of the computations to be presented later.

The q–f formulation

According to the q–f formulation, eqautions (4)–(6) are replaced by

$$\mu_T/Re = ql, \tag{18}$$

$$l = C_\mu |q|/f, \tag{19}$$

$$2u_m \frac{\partial q}{\partial x_m} - \frac{1}{x_2^\alpha}\frac{\partial}{\partial x_m}\left(x_2^\alpha \pi_q \frac{\partial K}{\partial x_m}\right) = P_q - D_q, \tag{20}$$

$$u_m \frac{\partial f}{\partial x_m} - \frac{1}{x_2^\alpha}\frac{\partial}{\partial x_m}\left(x_2^\alpha \pi_f \frac{\partial F'}{\partial x_m}\right) = P_f - D_f + R_f, \tag{21}$$

$$\pi_q = l/\sigma_q, \quad \pi_f = C_\mu q^2/2\sigma_f, \tag{22}$$

$$P_q = l\left[S_u + \frac{2}{\sigma_q}\left(\frac{\partial q}{\partial x_m}\right)^2\right], \quad P_f = C_\mu C_{1f} S_u \tag{23}$$

$$D_q = C_\mu q^2/l, \quad D_f = C_{2f} f^2, \tag{24}$$

where K and F' represent q^2 and $\ln f^2$ respectively. When R_f is set to zero, equations (18)–(24) will be said to constitute the q–f model of turbulence (as shown later, R_f can be chosen to render the system equivalent to k–ε). The currently favoured GFE discretization of this system, as described in Reference 21, differs in detail from that originally proposed in Reference 15 (particularly in the treatment of S_u) and is effected as follows. On each element q in the convective and K in the diffusive terms of equation (20) are interpolated on the same level as **u**. The source terms P_q and D_q are interpolated quadratically, whereas π_q is represented on the same level as pressure (i.e., linearly). Linear representations for S_u and $(\partial q/\partial x_m)^2$ are constructed on each element, these being defined by the values of these quantities at the Gauss points. An algebraic system for each element is then developed from equation (20) by weighting the residual with the velocity basis functions, the required nodal values of P_q, D_q and π_q being generated by evaluating equations (22)–(24) at each node (nodal values of S_u and $(\partial q/\partial x_m)^2$ are provided from their linear representations). The f equation (equation (21)) is treated similarly, with f in the convective and F in the diffusive terms interpolated on the same level as **u**.

The boundary conditions used are the counterparts of those discussed previously and apart from the wall treatment require little further explanation. At the wall $(\partial q/\partial n)_h = 0$ is applied as a natural boundary condition, equation (12) becomes $u_\tau = C_\mu^{1/4} q_h$ and f is evaluated as $C_\mu^{1/2} u_\tau/\kappa h$.

The resulting numerical model displays some very desirable features due to the properties of equations (18)–(24). These can be summarized as follows.

(i) The coupling between equations (20) and (21) is comparatively weak. Equation (20) depends upon f only through the definition of l (equation (19) and equation (21)) depends upon q only in the diffusivity π_f.

(ii) If equations (20) and (21) are viewed in separation (i.e., l is supplied to equation (20) and q^2 is supplied to equation (21)), then diffusivities remain positive (equation (22)) and sources and sinks do not reverse their role (equations (23) and (24)), irrespective of the sign of the dependent variables q and f.

(iii) If the first term of equation (20) is ignored, P_q is assumed given (by some previous iteration say) and suitable boundary conditions are supplied, then the discrete counterpart of the resulting equation has a unique solution for q^2. This immediately follows from linearity in q^2 and (ii) above. Smith[15] has demonstrated a similar result for equation (21) for a single one-dimensional element.

Property (iii) gives rise to the hope that equation (20) will yield a unique solution for q^2 and equation (21) a unique solution for f^2 under most practical conditions. Property (ii) suggests that an iterative scheme such as Newton–Raphson will not 'jump' to a non-physical regime and thus will fairly readily seek these solutions. Property (i) indicates that a cycling strategy which alternates between equations (20) and (21) should converge rapidly provided only a weak coupling is introduced at the boundaries. Thus a solution procedure is adopted which produces **u** from the momentum equations for a given μ_T; then, freezing **u** updates μ_T by cycling around equations (20) and (21).[15]

Generally speaking, these expectations are realised in practice and the scheme proves fairly robust. The main qualification arises from the fact that, due to the form of the convective terms in

equations (20) and (21), solutions are sought for q and f rather than q^2 and f^2. It is found that, if the grid is locally inadequate to capture the true variation, the expected solutions for q^2 and f^2 may overshoot to produce negative values, so that, locally, there is no real solution for the iterated variables q and f. In practice, this results in a local oscillation between iterations, the rest of the field being satisfactorily converged. In the true spirit of GFE, this is a sign that local refinement is required to capture local detail.

A set of values for the model constants has been produced with which the q–f model accurately simulates flow in a pipe expansion.[15] However, unlike k–ε, the model has not been benchmarked for a wide variety of flows, so that it cannot as yet be used with confidence in general application. If R_f in equation (21) is given by

$$R_f = R_{f\varepsilon} \equiv R'_{f\varepsilon} - \frac{1}{x_2^{\alpha}} \frac{\partial}{\partial x_m} \left(x_2^{\alpha} C_{\mu} \left(\frac{1}{\sigma_q} - \frac{1}{\sigma_f} \right) \frac{\partial K}{\partial x_m} \right), \tag{25}$$

where

$$R'_{f\varepsilon} = \frac{1}{2} C_{\mu} \left(\frac{1}{\sigma_q} + \frac{1}{\sigma_f} \right) \frac{\partial F'}{\partial x_m} \frac{\partial K}{\partial x_m} - C_{\mu} \left(\frac{1}{\sigma_q} - \frac{1}{\sigma_f} \right) \frac{\partial K'}{\partial x_m} \frac{\partial K}{\partial x_m} \tag{26}$$

and $K' = \ln q^2$, then the q–f system is formally equivalent to k–ε provided $C_{\mu}, \sigma_q, \sigma_f, C_{1f}, C_{2f}$ are given the values 0·09, 1·0, 1·3, 0·44, 0·92 respectively.[15] It is found that, if R_f is incorporated into the q–f formulation by discretizing $R'_{f\varepsilon}$ (equation (26)) in the same way as S_u and treating the diffusion term in equation (25) in the usual GFE fashion, the scheme's performance is only marginally affected and readily converges for many practical applications. Convergence can be aided by adding a streamline diffusion term to equations (20) and (21) in the manner of Hughes and Brooks,[35] but this is necessary only in the most difficult of cases. In view of the previous discussion concerning the difficulties in converging k–ε, this result may appear somewhat surprising but it is not contradictory. The choice of S_u and $R_{f\varepsilon}$ on the grid (linear and discontinuous between elements) guarantees a solution to the system for most practial configurations and the q–f formulation simply provides a stable route for locating it. In the cases where the gridding is not sufficient to yield a solution, the scheme fails only locally and in a mild manner, indicating where extra refinement should be introduced.

INDUSTRIAL APPLICATIONS USING THE q–f FORMULATION

The k–ε version of the above-described q–f-based scheme has been applied to a variety of industrial problems. Several of these are briefly described below, each highlighting one or more of the 'second-generation' features of the FEM listed in the Introduction. In each case the computations were performed on an IBM3081.

Gas flow in the boiler of an advanced gas-cooled reactor

The mesh shown in Figure 2(*a*) amply demonstrates the boundary-fitting capability of finite elements and the use of local refinement to resolve detail in regions of the flow where large gradients of the variables occur. The mesh was used to calculate cross-flow over boiler pipes in a symmetry element of the primary superheater of a nuclear boiler. The predicted flow streamlines and the turbulence energy field (non-dimensionalized) are shown in Figures 2(*b*) and 2(*c*) (u_b is the mean bulk velocity and D is the tube diameter) and they prove to be in reasonable agreement with available experimental data. Starting from an initial guess of $\mathbf{u} = \mathbf{0}$ and μ_T, l specified constants, convergence of the solution was obtained after 25 NR iterations of each equation set. Computing

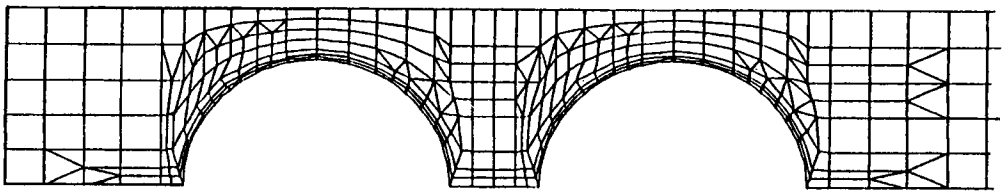

Figure 2(*a*). Finite element mesh (467 elements) for flow over AGR boiler pipes

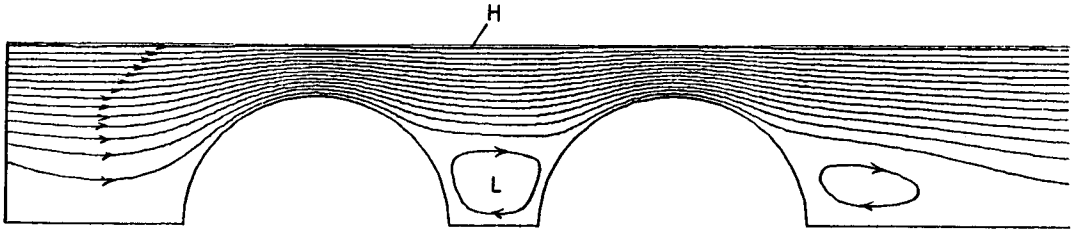

Figure 2(*b*). Flow over AGR boiler pipes; stream function ($\psi/u_b D$). Contours equally spaced, $L = -0{\cdot}0196$, $H = 0{\cdot}66$

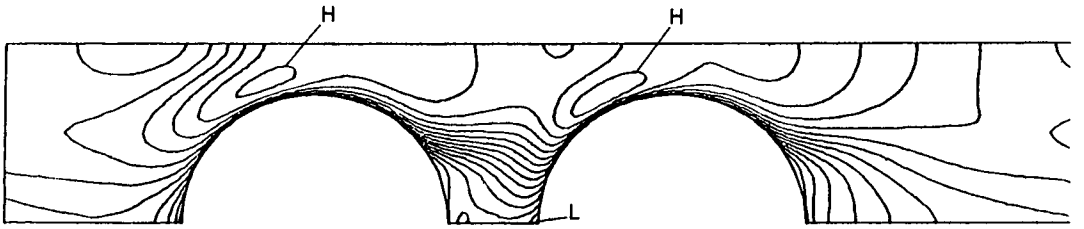

Figure 2(*c*). Flow over AGR boiler pipes; (turbulence energy)$^{1/2}$ (i.e. q/u_b). Contours equally spaced, $L \equiv 0{\cdot}177$, $H \equiv 0{\cdot}902$

times for one NR iteration of the momentum, q and f sets of equation were 10·5, 3·8 and 4·9 respectively.

Electromagnetic stirring of a coreless induction furnace

In Figure 3(*a*), a finite element prediction[37] of the flow field in an axisymmetric model of an induction furnace is compared with experiment. The body force in this flow arises from the interaction of the induced current and magnetic field from a coil wrapped around the furnace. Figure 3(*b*) shows profiles of vertical velocity across the centre of the upper vortex and agreement between experiment and the finite element prediction can be seen to be quite good. In comparison, a published prediction obtained using a conventional finite volume code badly underpredicts the vortex strength, almost certainly due to numerical errors on an inadequate mesh. The finite element prediction shows that the discrepancy between experiment and the finite volume solution is not due to the k–ε turbulence model as previously supposed. The finite element mesh consisted of 22 × 13 rectangular elements and each NR iteration of the momentum, q and f equation sets took 14·6, 3·9 and 3·9 s respectively. Convergence of the solution was obtained after 30 NR iterations of each equation set, using a simple initial guess of $\mathbf{u} = \mathbf{0}$ and μ_T, l specified constants.

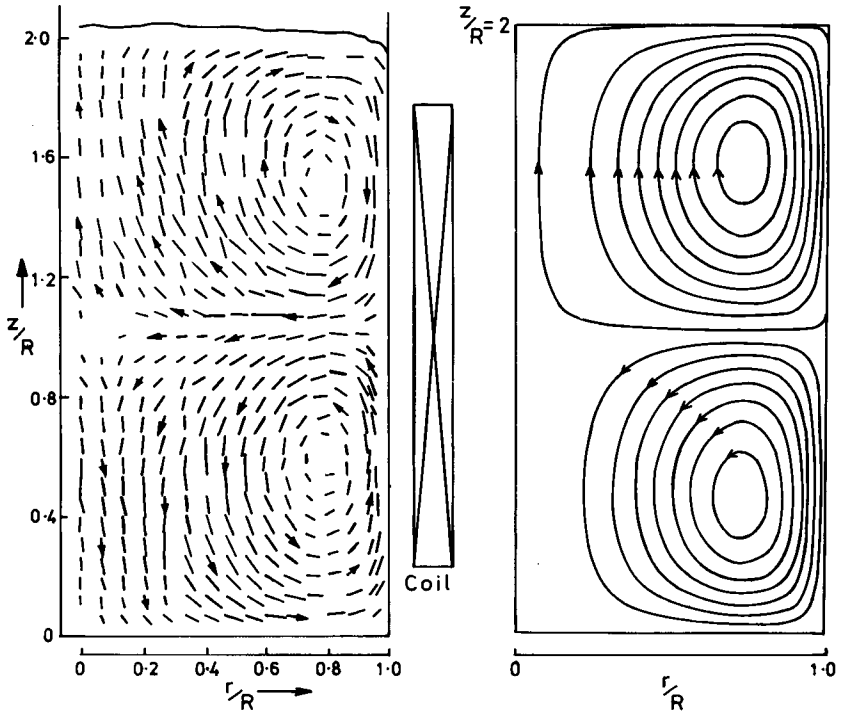

Figure 3(*a*). Coreless induction furnace; comparison of experimental velocity vectors with the finite-element-predicted streamline pattern

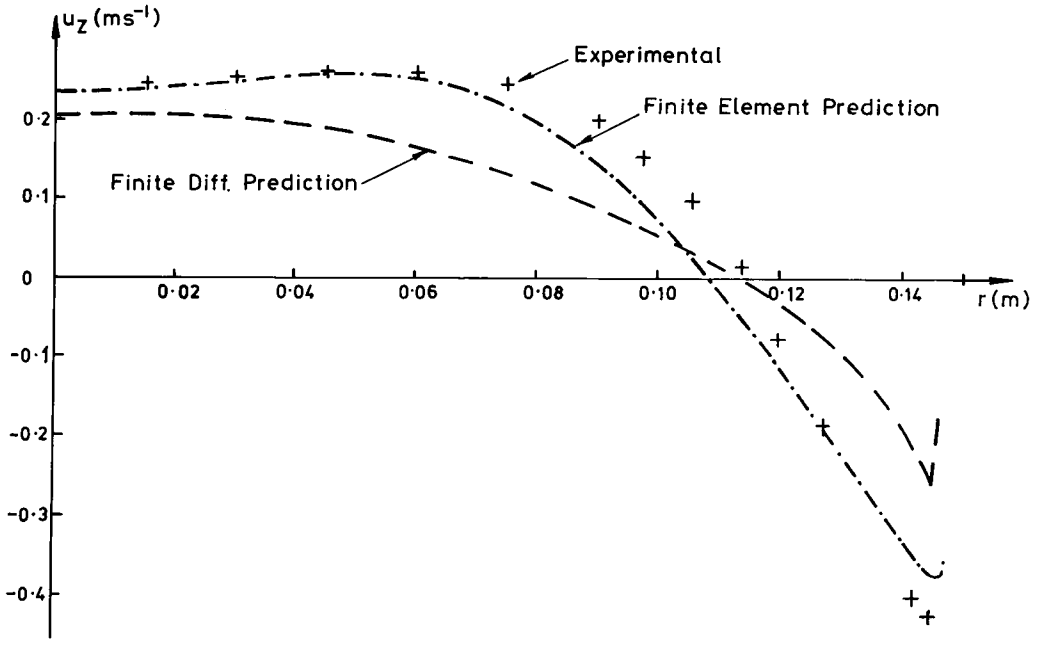

Figure 3(*b*). Coreless induction furnace; comparison of computed and experimental vertical velocity profiles along a radius through the centre of the upper eddy

Gas jet penetration into a large building

Figure 4(*a*) represents an axisymmetric idealization of jet penetration into a large building. A gas jet emerges from a cylindrical vessel situated below the floor of the building and entrains air drawn through a surrounding annulus before passing into the building through a floor aperture. The jet impinges on the roof, circulates around the building and then exits through the floor vent at A. This application exemplifies how topologically non-structured grids can be used to match two regions differing greatly in scale. The grid used consists of 569 elements and 1720 nodes. Each NR iteration of the momentum, q and f equation sets took 19, 4 and 5 s respectively. Due to the complexity of the flow, a certain amount of coaxing was necessary to gain a solution from a zero-velocity, constant-μ_T initialisation. However, once obtained, it served as a starting point for subsequent runs, which converged in 10–20 NR iterations of each set.

The aim of the exercise is to predict the variation of pressure drop, Δp, across the floor with entrainment ratio λ (mass flow drawn through the annulus divided by jet mass flow at the nozzle). This pressure drop can be varied in practice by opening or closing the vent A. Figures 4(*b*) and 4(*c*) show the entrainment flow patterns for a high and low Δp respectively. The required Δp–λ variation (Δp normalized against ρU^2, where U is the jet velocity at the nozzle) is given in Figure 5. The broken curve represents the standard k–ε prediction, whereas the chain curve represents the prediction with $C_{1\varepsilon}$ increased to 1·6. This modification is known to correct the round jet anomaly (i.e., reduce entrainment into a free round jet to the observed value)[38] and, as can be seen, brings the present prediction into much closer agreement with experiment.

Turbulent flow in an electrostatic precipitator

The fluid flow code incorporating the q–f algorithm has been extended to include the equations governing the electric field and transport of charge in an electrostatic precipitator. This enables the simulation of the turbulent flow within the precipitator and, in particular, its response to the electrostatic force field. Figure 6(*a*) portrays the configuration and grid used for one such calculation. The region of interest is a 300 mm wide channel with earthed walls and a series of strip electrodes arranged along the centre of the channel, each having one edge serrated to promote a discharge in its vicinity. It is evident that a non-structured grid such as that shown is required to practically resolve the detail of this discharge and the associated field. Figure 6(*b*) shows the calculated contours of electric potential and charge density within the precipitator when the average current density across the earth-plate is 100 μA m^{-2} and the discharge is oriented to the right. The response of the flow to the electrostatic force field is shown in Figure 6(*c*), where both the axial velocity and q-profiles across the channel at a location midway between electrodes are plotted. It can be seen that the flow in the centre of the channel is accelerated in the direction of the discharge and turbulence levels are increased generally.

CHALLENGES AND PROSPECTS FOR THE FUTURE

It is clear that activity in turbulent flow simulation is now burgeoning and that several approaches have recently evolved which render the finite element method fully capable of solving two-dimensional turbulent flows of industrial complexity. That is to say, solutions to the k–ε system in complex configurations can be attained without painful coaxing and operator intervention and with only modest demands upon computer time and memory. Furthermore, the simulations which have so far been performed have highlighted to great effect the virtuosity of the method in this important field of CFD. What, then, are the challenges and prospects for the future?

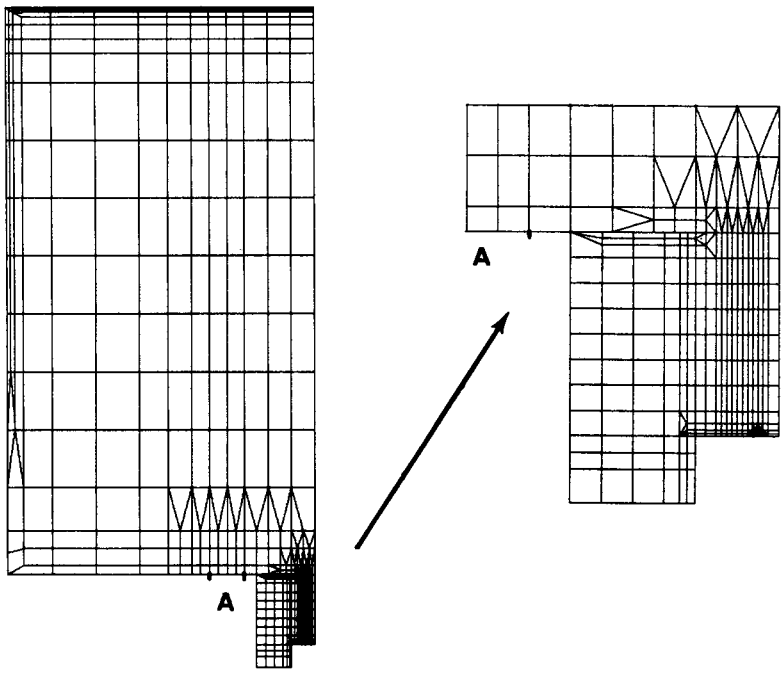

Figure 4(*a*). FE grid for gas jet penetration into a large building

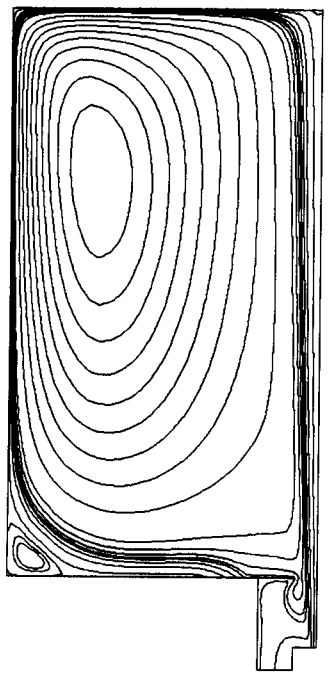

Figure 4(*b*). Gas jet penetration into a large building; streamlines for high Δp

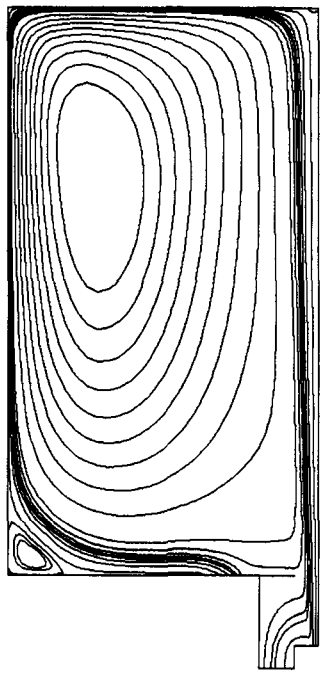

Figure 4(*c*). Gas Jet penetration into a large building; steamlines for low Δp

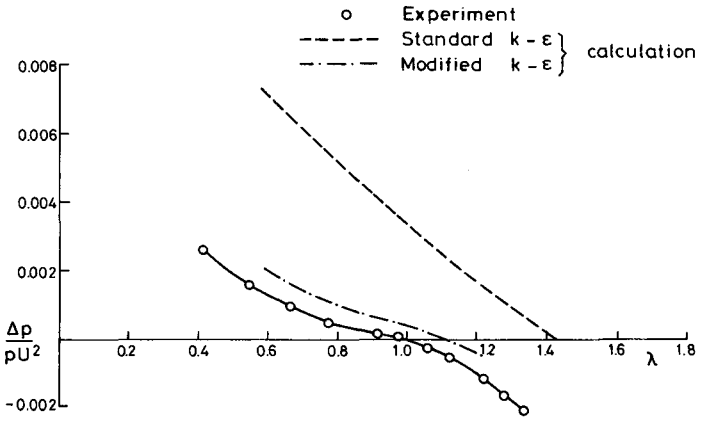

Figure 5. Gas jet penetration into a large building; comparison between experiment and calculation

One of the unique advantages of the FEM is the use of non-structured grids in resolving local detail. This advantage, while attractive in two dimensions, could be crucial for the effective design of three-dimensional grids to fit difficult geometries. Baker and Jameson in a recent article[12] point out the difficulty of designing finite-volume-type structured grids (i.e., a grid of regular topology) to fit complex three-dimensional geometries. In their opinion, this difficulty has hindered the development of flow field computational methods to treat a complete aircraft and they are currently developing an approach based upon non-structured grids of tetrahedra. Thus, if the finite element method is to realize its true potential in industrial application, any turbulent flow

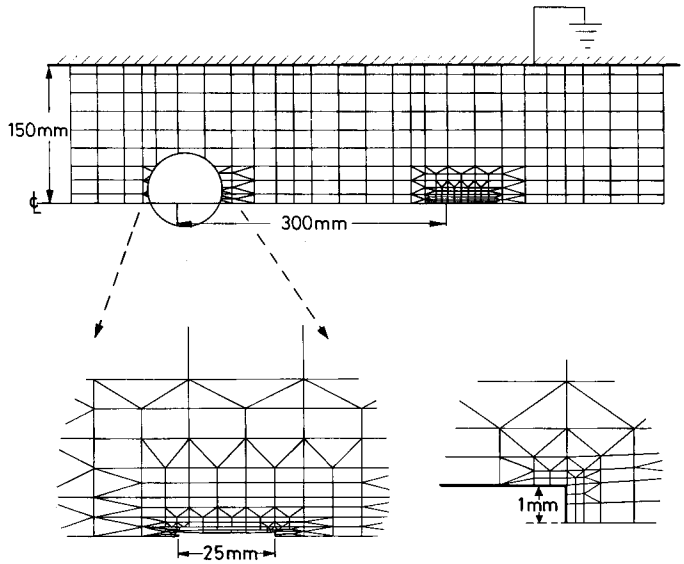

Figure 6(*a*). Turbulent flow in an electrostatic precipitator; configuration and grid

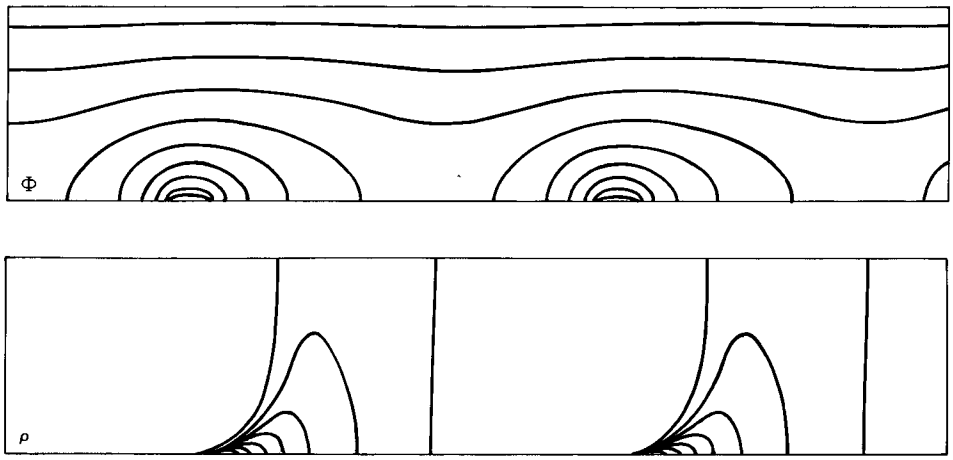

Figure 6(*b*). Turbulent flow in an electrostatic precipitator; calculated contours of electric potential (Φ) and charge density (ρ)

capability must be viable (i.e., considered affordable) on practical, three-dimensional grids of general design. This poses a far from trivial challenge, as can be appreciated by considering the costs of treating a regular, linear brick grid with N nodes in each of the three co-ordinate directions. If the steady equations are tackled directly, then, as we have seen, the method is likely to alternate between turbulence and momentum sets, updating each perhaps by a combination of NR iteration and direct elimination (e.g., a frontal solver) within each iteration. If it is assumed that, in order to reduce costs, pressure is eliminated by employing a penalty treatment of continuity, then for each momentum update (of which there could be many) the operation count per NR iteration (excluding assembly) is $\sim 54N^7$ (cf. $16N^4$ in 2D) and the storage requirement is $\sim 9N^4(N+1)$ (cf. $4N^2(N+1)$ in 2D). Thus, for example, if N is 30, which is by no means overtaxing for FV codes, the number of operations per NR iteration is $\sim 10^{12}$ and the storage requirement is 226

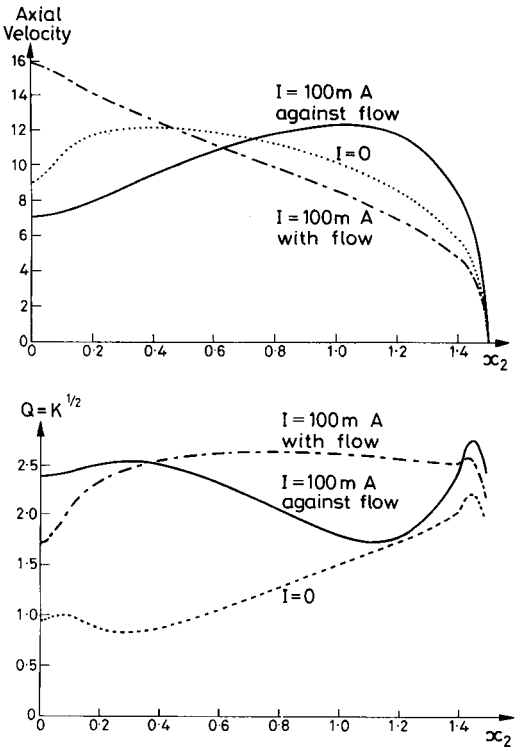

Figure 6(*c*). Turbulent flow in an electrostatic precipitator; profiles of axial velocity and q across the channel midway between electrodes for various discharge orientations

megawords. In most industrial environments this would be considered unaffordable. It would therefore seem that more explicit, iterative algorithms are required which can separate the nodal variables both in type and in space, reducing the scale of the problem to manageable proportions. Indeed, such algorithms lie at the heart of most FV codes. In the FE context, if the advantage of non-structured grids is to be retained, this is perhaps simpler to contrive by tackling the transient equations and time-stepping to the steady state. The problems of affordable time-dependent solutions to the three-dimensional Navier–Stokes equations have been examined in some depth by Gresho *et al.*[19] Their three-dimensional explicit algorithm[30] has evolved out of these studies and this has been adapted for turbulent flow computation by Betts and Haroutunian.[29] While this undoubtedly represents a significant advance, unfortunately the stability limit on the Courant number must lead to an impairment of the local refinement capability (and hence arbitrary grid design), which is the major attraction in three dimensions.*

The semi-implicit characteristic–Galerkin technique being pursued by the Group at Electricité de France–LNH, being unconditionally stable, does not suffer any such practical limitation. Each nodal variable (including each velocity component) is treated separately and only fairly simple Poisson systems (amenable to conjugate gradient solution) are handled each time step. The method has been demonstrated for various two-dimensional turbulent flows as well as for a three-

*It has been pointed out to the authors that, using the later, semi-implicit version of the Gresho *et al.* algorithm,[41] this impairment is not so severe. The Courant number stability limit is significantly relaxed ($C \lesssim 5$ to 10) whereas the diffusion limit, which may be more restrictive if the local refinement is introduced to capture regions of high shear, is removed completely.

dimensional laminar flow on a complex, non-structured grid (12936 quadratic tetrahedra, 20108 nodes).[39] The latter was performed upon a CRAY XMP requiring 20 min of CPU time and 2·5 megawords of memory.

Progress, then, is being made on affordable extension to three dimensions and, given the upturn in activity generally in FE turbulent flow computation and a growing realization of its advantages in 3D, new, innovative ideas are sure to emerge in the near future. The much more daunting challenge for the future, one which faces all workers in the field, whether finite element or finite volume, is the improvement of the underlying physical models. It is now conceded that wall functions are valid only for a very limited range of conditions, essentially when the turbulence structure is in local equilibrium and far-field influences are of secondary importance. If these functions are to be abandoned, then effective means must be evolved for coping with the large number of grid points which must by necessity be introduced in the neighbourhood of the wall. With the exception of Taylor *et al.*[40], it seems very little (finite-element-based) effort is being devoted to this problem. The k–ε turbulence model itself is also of fairly limited applicability, particularly if details of the turbulence field are important (it may hold up quite well for gross features of the flow). The thrust forward is to move to algebraic stress or perhaps full Reynolds stress transport models for which five (in 2D) or seven (in 3D) highly coupled, non-linear (temperamental) equations for the turbulence field have to be solved. It seems probable that routine industrial flow simulation will rely on k–ε and wall functions for some time to come.

ACKNOWLEDGEMENT

This paper is published by permission of the Central Electricity Generating Board.

REFERENCES

1. O. C. Zienkiewicz, R. Loehner, K. Morgan and S. Nakazawa, in R. H. Gallagher, J. T. Oden, O. C. Zienkiewicz, T. Kawai and M. Kawahara (eds), *Finite Elements in Fluids, Vol. 5*, Wiley Chichester and New York, 1984.
2. C. Taylor, M. D. Olson, P. M. Gresho and W. G. Habashi (eds), *Numerical Methods in Laminar and Turbulent Flow*, Pineridge Press, Swansea, 1985.
3. T. Kawai (ed.), *Finite Element Flow Analysis*, North-Holland, Amsterdam, 1982.
4. M. O. Bristeau, R. Glowinski, A. Hauguel and J. Periaux (eds), *Proc. Sixth Int. Symp. on Finite Element Methods in Flow Problems*, Antibes, France, INRIA, 1986.
5. A. G. Hutton, 'Current progress in the simulation of turbulent incompressible flow by the finite element method', in C. Taylor, M. D. Olson, P. M. Gresho and W. G. Habashi (eds), *Numerical Methods in Laminar and Turbulent Flow*, Pineridge Press, Swansea, 1985.
6. B. E. Larock and D. R. Schamber, 'Approaches to the finite element solution of two-dimensional turbulent flows', in C. Taylor and K. Morgan (eds), *Computational Techniques in Transient and Turbulent Flow*, Pineridge Press, Swansea, 1981.
7. G. D. Tong, 'Computation of recirculating flows in two-dimensions using finite elements and the k–ε model', *Proc. First IAHR Symp. on Refined Modelling of Flows*, Pressés de l'Ecole Nationale des Ponts et Chaussées, Paris, 1982.
8. R. M. Smith, 'On the finite element calculation of turbulent flow using the k–ε model', *Int. j. numer. methods fluids*, **4**, 303–320 (1984).
9. G. F. Polansky, J. P. Lamb and M. E. Crawford, 'A finite element analysis of incompressible turbulent backstep flow with heat transfer', *AIAA 2nd Aerospace Sciences Meeting, AIAA Paper No. 84-0178*, 1984.
10. A. Autret, 'Calculs d'ecoulements turbulents par une methode aux elements finis vols 1 and 2', *Centre d'Etudes Nucleaires de Cadarache, France, Note CEA-N-2474*, 1986.
11. J. G. Rice and R. J. Schnipke, 'An efficient finite element method for viscous fluid flows', in C. Taylor, M. D. Olson, P. M. Gresho and W. G. Habashi (eds), *Numerical Methods in Laminar and Turbulent Flow*, Pineridge Press, Swansea, 1985.
12. T. Baker and A. Jameson, 'Computational methods and aerodynamics', *Cray Channels, No. 8*, Cray Research, Summer 1986.
13. W. Rodi, 'The modelling of turbulent flows using transport equation models', *Proc. First IAHR Symp. on Refined Modelling of Flows*, Pressés de l'Ecole Nationale des Ponts et Chaussées, Paris, 1982.
14. A. J. Baker and J. A. Orzechowski, 'An interaction algorithm for three-dimensional turbulent subsonic aerodynamic juncture region flow', *AIAA J.*, **21**, 524–533 (1983).

15. R. M. Smith, 'A practical method of two-equation turbulence modelling using finite elements', *Int. j. numer. methods fluids*, **4**, 321–336 (1984).
16. A. C. Benim and W. Zinser, 'Investigation into the finite element analysis of confined turbulent flows using a k–ε model of turbulence', *Comput. Methods Appl. Mech. Eng.*, **51**, 507–523 (1985).
17. C. Taylor, C. E. Thomas and K. Morgan, 'Modelling flow over a backward-facing step using the FEM and the two-equation model of turbulence', *Int. j. numer. methods fluids*, **1**, 295–304 (1981).
18. P. M. Gresho and R. L. Lee, 'Don't suppress the wiggles—they're telling you something!', *Comput. Fluids*, **9**, 223–254 (1981).
19. P. M. Gresho, R. L. Lee and R. L. Sani, 'On the time dependent solution of the incompressible Navier–Stokes equations in two and three dimensions', in C. Taylor and K. Morgan (eds), *Recent Advances in Numerical Methods in Fluids, Vol. 1*, Pineridge Press, Swansea, 1980.
20. M. S. Engelman, R. L. Sani, P. M. Gresho and M. Bercovier, 'Consistent vs. reduced integration penalty methods for incompressible media using several old and new elements', *Int. j. numer. methods fluids*, **2**, 25–42 (1982).
21. R. M. Smith, 'The current status of turbulence modelling in the fluid flow code FEAT, January 1985', CEGB Report T PRD/*B*/0591/*N85*, 1985.
22. A. G. Hutton and R. M. Smith, 'On the finite element simulation of incompressible turbulent flow in general two-dimensional geometries', in C. Taylor and B. A. Schrefler (eds), *Numerical Methods in Laminar and Turbulent Flow*, Pineridge Press, Swansea, 1981.
23. K. Morgan, T. G. Hughes and C. Taylor, 'The analysis of turbulent, free-shear and channel flow by the finite element method', *Comput. Meth. Appl. Mech. Eng.*, **19**, 117–125 (1979).
24. B. A. Devantier and B. E. Larock, 'Modelling a recirculating density-driven turbulent flow', *Int. j. numer. methods fluids*, **6**, 241–254 (1986).
25. H. Uchida, 'Finite element analysis of two-equation model of turbulent flow through ducts of complicated geometry', *Ph.D. Thesis, University of Tokyo*, 1985.
26. C. Deschenes, G. Dhatt, D. Nguyen, 'Simulation d'écoulements turbulents dans un labyrinthe bi-dimensionnel', *Proc. Sixth Int. Symp. on Finite Element Methods in Flow Problems*, Antibes, France, INRIA, 1986.
27. A. J. Baker, *Finite element computational fluid mechanics*, Hemisphere, 1983.
28. L. P. Hackman, G. D. Raithby and A. B. Strong, 'Numerical predictions of flows over backward-facing steps', *Int. j. numer. methods fluids*, **4**, 711–724 (1984).
29. P. L. Betts and V. Haroutunian, 'k–ε modelling of turbulent flow over a backward facing step by a finite element method. Comparison with finite volume solutions and experiment', in C. Taylor, M. D. Olson, P. M. Gresho and W. G. Habashi (eds), *Numerical Methods in Laminar and Turbulent Flow*, Pineridge Press, Swansea, 1985.
30. P. Gresho, S. Chan, R. Lee and C. Upson, 'A modified finite element method for solving the time dependent, incompressible Navier–Stokes equations', *Int. j. numer. methods fluids*, **4**, 557–598 (*Part 1: Theory*), 619–640 (*Part 2–Applications*) (1984).
31. J. P. Benquè, G. Labadie and J. Ronat, 'A new finite element method for Navier–Stokes equations, coupled with a temperature equation', in T. Kawai (ed.), *Finite Element Flow Analysis*, University of Tokyo Press and North-Holland, Amsterdam, 1982.
32. J. Goussebaile, A. Jacomy, A. Hauguel and J. P. Grégoire, 'A finite element algorithm for turbulent flow processing a k–ε model', in C. Taylor, M. D. Olson, P. M. Gresho and W. G. Habashi (eds), *Numerical Method in Laminar and Turbulent Flow*, Pineridge Press, Swansea, 1985.
33. J. F. Brison, M. Buffat, D. Jeandel and E. Serres, 'Finite element simulation of turbulent flows, using a two-equation model', in C. Taylor, M. D. Olson, P. M. Gresho and W. G. Habashi (eds), *Numerical Methods in Laminar and Turbulent Flow*, Pineridge Press, Swansea, 1985.
34. G. Brun, M. Buffat, D. Jeandel and E. Serres, 'Finite element simulation of turbulent variable density fluid flows', *Proc. Sixth Int. Symp. on Finite Element Methods in Flow Problems*, Antibes, France, INRIA, 1986.
35. T. J. R. Hughes and A. Brooks, 'A multi-dimensional upwind scheme with no cross-wind diffusion', in T. J. R. Hughes (ed.), *Finite element methods for convection dominated flows, AMD Vol. 34*, ASME, New York, 1979.
36. N. Coulon and J. P. Magnaud, 'Contribution TRIO au cas test AIRH-11', *Communication to the 11th Meeting of the IAHR Working Group on Refined Modelling of Flows*, Berkeley Nuclear Laboratories, May 1986.
37. R. M. Smith, 'A prediction of liquid metal flow in a coreless induction furnace by the finite element method', *CEGB Report TPRD/B/0589/N85*, 1985.
38. S. B. Pope, 'An explanation of the turbulent round-jet/plane-jet anomaly', *AIAA J.*, **16**, 279–281 (1978).
39. P. Lasbleiz, J. P. Chabard, J. P. Grégoire, O. Daubert, J. Goussebaile and P. H. Hemmerich, 'Efficient computation of 3D industrial turbulent flow by finite element method', *Proc. Sixth Int. Symp. on Finite Element Methods in Flow Problems*, Antibes, France, INRIA, 1986.
40. C. Taylor, A. A. Gheissary and J. O. Medwell, 'A note on the replacement of universal profiles in near wall zones using the finite element method', in C. Taylor, M. D. Olson, P. M. Gresho and W. G. Habashi (eds), *Numerical Methods in Laminar and Turbulent Flow*, Pineridge Press, Swansea, 1985.
41. P. M. Gresho and S. T. Chan, 'A new semi-implicit method for solving the time dependent conservation equations for incompressible flows', in C. Taylor, M. D. Olson, P. M. Gresho and W. G. Habashi (eds), *Numerical Methods in Laminar and Turbulent Flow*, Pineridge Press, Swansea, 1985.